Effects of a Magnetic Field on Nuclear Spin Ordering in Solid ^{3}He†

R. B. Kummer, E. D. Adams, W. P. Kirk, A. S. Greenberg,* R. M. Mueller, C. V. Britton, and D. M. Lee‡
Physics Department, University of Florida, Gainesville, Florida 32611
(Received 30 December 1974)

The effects of applied magnetic field up to 1.2 T have been observed on nuclear spin ordering in solid He. For B 0.4 T the transition is sharp and is depressed in temperature by the field. For $B \geq 0.42$ the ordering region is broadened and moves to significantly higher temperatures with increasing fields.

For many years nuclear spin ordering in solid ^{3}He has been one of the outstanding problems in low-temperature physics. Until a few years ago, existing experiments in the high-T limit above the expected ordering temperature indicated an antiferromagnetic transition at $T_N = 2.0$ mK (for the melting solid).[1] However, several recent experiments[2-4] have given results which cannot be understood with the Heisenberg nearest-neighbor model, and interest in the problem has become more intense. The results of Halperin *et al.*[4] indicate a transition at 1.17 instead of 2.0 mK. Whether the transition is antiferromagnetic, as expected from high-T experiments, has not been established.

In order to provide additional information on the nature of the transition, we have studied the ordering in applied magnetic fields up to 1.2 T. We find that for fields up to 0.4 T the transition remains sharp (i.e., covers a narrow temperature interval) and is depressed in temperature by the field. At 0.42 T and above the ordering region is broadened and *moves to higher temperatures* with increasing fields. For 1.2 T the ordering temperature has increased to 1.60 mK.

A mixture of liquid and solid ^{3}He was cooled along the melting curve using adiabatic compression.[5] The Pomeranchuk compression cell was cylindrical in shape with the displaceable wall being a stressed brass tube 2.44 cm in diameter, 10.80 cm long, with a wall thickness of 0.015 cm. Increasing the ^{4}He pressure inside a coaxial cylindrical space around this tube produced the required change in volume. Most of the volume inside the tube was excluded, leaving a volume of 5.7 cm^3 for ^{3}He. The cell was equipped with capacitive pressure gauges[6] for measuring the ^{3}He pressure $P_3 = P$ and the ^{4}He pressure P_4. Changes in the volume of the cell could be determined by measuring the change of $P_3 - P_4$. The cell contained a heater constructed of 4000 cm of 0.0025-cm-diam copper wire occupying (randomly) a volume of 2.4 cm^3. The entire cell was placed inside a sixth-order compensated superconducting solenoid for providing the magnetic field.

The method which we have used to study the solid ordering is essentially the same as that of Halperin *et al.*[4] With the temperature held constant by the appropriate compression rate, an amount of heat ΔQ is added to the liquid and solid ^{3}He mixture, causing a change in volume ΔV as liquid is converted to solid. The quantities ΔQ and ΔV are measured as a function of the melting pressure P. In order to determine the temperature, use is made of the Clausius-Clapeyron equation, $dP/dT = \Delta S/\Delta V = \Delta Q/(T\Delta V)$, to obtain

$$\int_{T_0}^{T} T^{-1} dT = \int_{P_0}^{P} (\Delta V/\Delta Q) dP,$$

where T_0 and P_0 are taken at a point where the melting pressure has been reasonably well established.[7] With $\Delta V/\Delta Q$ measured as a function of P, evaluation of the integral gives $T(P)$. Next the Clausius-Clapeyron equation is used to give the solid entropy $s_S(T)$, using the known behavior of the liquid entropy[8] and the molar volume change at melting ΔV.[7,9]

Two techniques for measuring $\Delta V/\Delta Q$ were used. With the first technique, used everywhere except very near the solid transition, the ^{4}He pressurization rate was automatically adjusted to maintain constant ^{3}He pressure and temperature shortly before, during, and after a pulse of heat. A typical chart trace of P_3 and P_4 versus time with this technique is shown in the inset of Fig. 1. During the pulse there are two contributions to ΔQ, the applied heat and that from heat leaks, with each of these contributing to ΔV. By extrapolation of $P_4(t)$ before and after the pulse to the center of the pulse the change in P_4 at the center gave ΔV corresponding to the applied ΔQ.

Because of the reduced cooling power near the

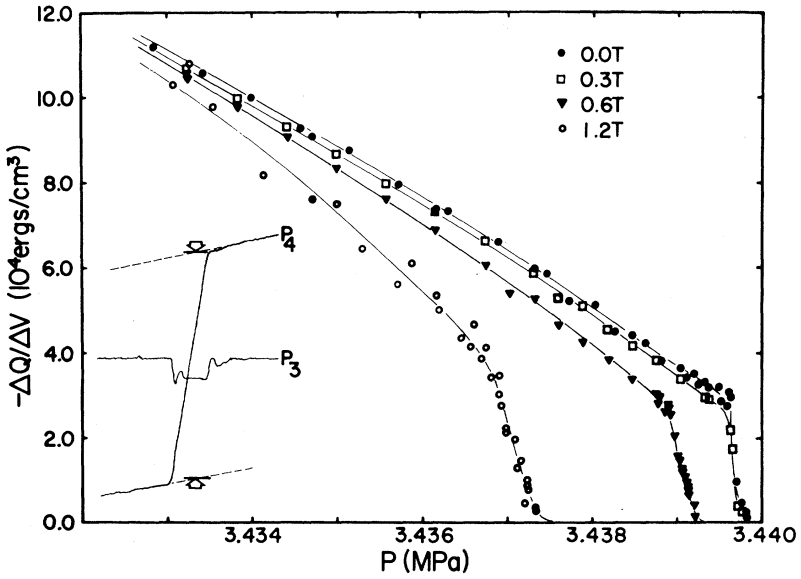

FIG. 1. Raw data $\Delta Q/\Delta V = T\,dP/dT$ versus P for various fields. The plot covers the region below about 3.0 mK. The lines are "eyeball" fits to the points and were used to generate the required density of points for the numerical integration. The inset shows a recorder tracing of P_3 and P_4 versus time during a heat pulse.

transition, compression rates were much higher and a second method was used. In this case a steady compression rate was used (for a particular ^{3}He pressure), giving a particular rate of change of V, $\dot{V}$. Then the applied heating rate was adjusted so as to produce a constant P_3 and T. The heat leak, measured over a range in T above the transition, was added to the applied heating rate $\dot{Q}_a$ to give the total $\dot{Q}$. In the analysis $\dot{Q}$ and $\dot{V}$ replace ΔQ and ΔV. Overlapping points taken by each method gave good consistency.

In Fig. 1 are plots of $T\,dP/dT$ versus P for different magnetic fields. As expected, in higher fields $T\,dP/dT$ falls gradually below that for lower fields. At low fields, a pressure is reached where $T\,dP/dT$ undergoes a rapid decrease with increasing pressure (this point is identified with the ordering temperature T_c). For $B \leq 0.4$ T there is essentially no change in the pressure where this occurs and the transition region remains very narrow. On going to 0.42 T this character has changed dramatically (apparently discontinuously for $0.4 < B < 0.42$ T), with the pressure at the ordering temperature now decreasing with increasing field and the ordering region becoming much broader.

From the data of Fig. 1, $T(P)$ and $s_S(T, B)$ were determined as discussed above. In Fig. 2 is shown $s_S(T, B)$ for several fields. In zero field our value of T_c is 1.03 mK. As a comparison of our overall temperature scale with that of others, we find the A and B' transitions in liquid ^{3}He to be at $T_A = 2.68$ mK and $T_{B'} = 2.10$ mK. We estimate the accuracy of our temperatures to be about 8% with the precision somewhat better than this. Our zero-field entropy has the same general shape, including the feature associated with the specific-heat bump near 2 mK, as that of Halperin *et al.*[4,7] However, in our case this precursory bump is not as pronounced and has a broader maximum at a somewhat lower temperature.

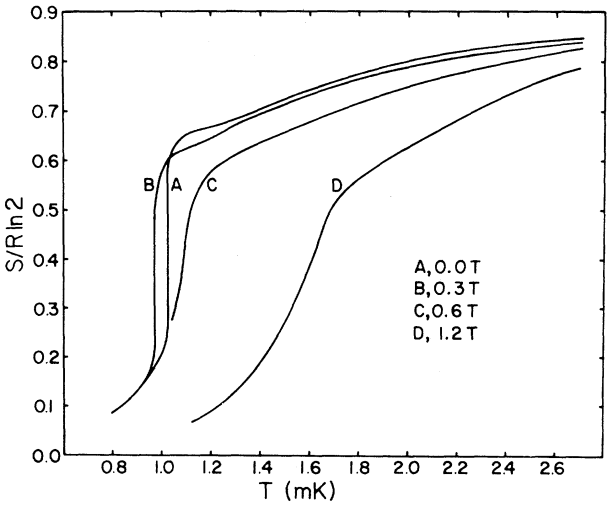

FIG. 2. Entropy versus temperature for various magnetic fields, as determined from the lines in Fig. 1.

Well above the transition, there is a decrease in the entropy in a field relative to that for zero field because of spin alignment by the field. For low fields the entropy drops precipitiously at $T_c \simeq 1$ mK. Upon increase of the field, T_c decreases for $B \leq 0.4$ T. The character of $s_S(T, B)$ is completely different for $B \geq 0.42$ T. Now the reduction in entropy occurs much more gradually, and the position of the ordering temperature defined by the maximum in the specific heat, $C = T \times dS/dT$, *moves up* in temperature with increasing fields. These conclusions are each related to the features of the $T\,dP/dT$ data of Fig. 1 and are supported qualitatively by these raw data.

The ordering temperature versus field is plotted in Fig. 3(a). Although a sufficient number of points have not yet been accumulated to show the detailed shape of the curves (each point requires about 10 days running time), it is clear that the low- and high-field points fall on two different branches. Another way of showing qualitatively that the character of the ordering has changed above 0.4 T is provided by Fig. 3(b). Here we plotted $P_{max}(0) - P_{max}(B)$ versus B^2, where P_{max} is the maximum melting pressure reached in the compression. Compressions have been performed in several fields between 0.3 and 0.6 T (for which $T\,dP/dT$ data are incomplete) to determine where the change from low-field to high-field behavior occurs. For $B \leq 0.40$ T, $P_{max}(0) - P_{max}(B) \simeq 0$, but at 0.42 T there is a rapid rise to the previously observed B^2 dependence of this quantity in higher fields.[10] A more dramatic change occurs in the "width" of the ordering region. This is a qualitative feature which we take here to be the difference in P_{max} for two particular compression rates differing by about a factor of 5. The inset of Fig. 3(b) shows the width versus B^2. There appears to be a discontinuous or very rapid change in width for $0.4 < B < 0.42$ T.

One interpretation of Fig. 3(a) is that the lower branch of the curve is the usual paramagnetic-to-antiferromagnetic boundary and that the upper branch is the paramagnetic–to–spin-flop boundary, with a spin-flop field $B_{SF} \simeq 0.42$ T. Using this interpretation, we estimate the anisotropy field B_A from the molecular-field expression[11] $B_{SF} = (2B_{AF}B_A - B_A^2)^{1/2}$, where B_{AF} is the antiferromagnetic exchange field given by $B_{AF} = 2z|J|I/\mu = 7.4$ T. With $B_{SF} = 0.42$ and $B_{AF} = 7.4$, Eq. (3) gives $B_A = 12$ mT. The expected source of anisotropy in solid ^{3}He is the dipolar field which leads to 0.3 nT for B_A and to $B_{SF} = 0.065$ mT.[11] In addition to the high anisotropy field indicated, another unexpected result is the large increase of transition temperature with increasing magnetic field for the upper branch of the solid-phase transition shown in Fig. 3(a). In electronic antiferromagnets a negative slope for this curve is more common.

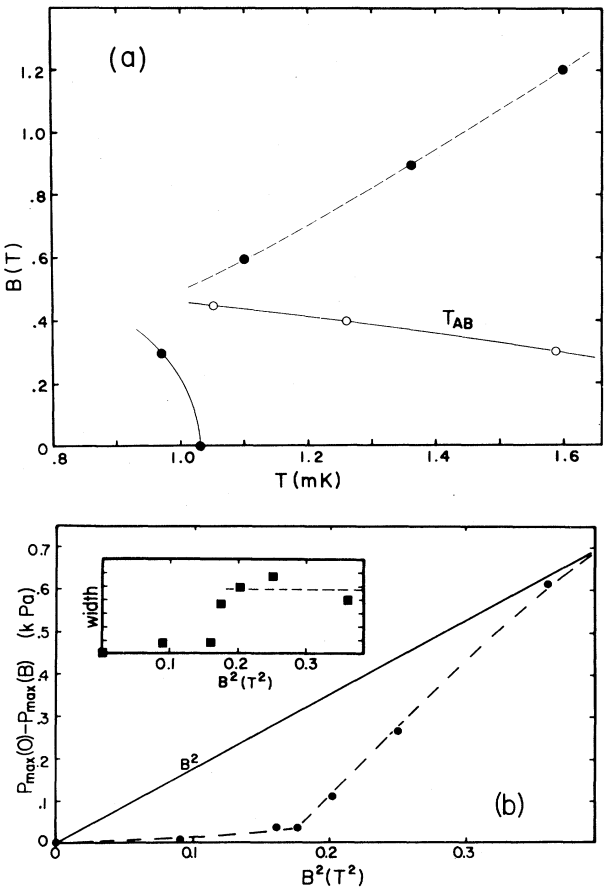

FIG. 3. (a) B-T phase diagram of the solid transition, closed circles. The detailed shape of the phase boundaries is not known; the lines are merely suggestive. The open circles show our location of the BA transition between the superfluid phases of liquid ^{3}He. (b) Field dependence of P_{max}, the maximum pressure reached in compression. The B^2 line shows the field dependence found at higher fields. Inset: "width" of the ordering region (relative scale) versus B^1.

A second interpretation of Fig. 3(a), which may be more likely, is that the lower branch is the paramagnetic–to–spin-flop (or antiferromagnetic) boundary and that the specific-heat peaks for higher fields do not indicate a transition but simply ordering by the applied field. (For $B = 1.2$ T, the shape of the entropy curve is vaguely similar to that for a noninteracting paramagnetic system in a field about twice the actual applied field.) With

this interpretation, the critical field for the ordered phase is probably an order of magnitude less than the expected antiferromagnetic critical field of 7.4 T.

Another curious feature seen in Fig. 3(a) is that the curve T_{AB} corresponding to the transition between the two superfluid phases of liquid ^{3}He seems to intersect the solid transition line about 0.45 T, very near the field at which the solid changes behavior. It is unknown whether this is a coincidence or whether there exists a relationship between the AB transition in liquid ^{3}He and the magnetic phase transition in solid ^{3}He. We believe that the latter possibility is unlikely, although it should be remarked that the measured quantities relate to phenomena occurring at the liquid-solid interface and that the bulk solid is not in thermal equilibrium with the liquid.

We gratefully acknowledge the expert advice and skillful machining of W. E. Steeger. Thanks are extended to P. L. Coleman for maintaining a continuous supply of helium since this run began in mid-September.

†Work supported in part by the National Science Foundation and the Research Corporation.

*Present address: Department of Physics, Colorado State University, Fort Collins, Colo. 80523

‡John Simon Guggenheim Memorial Fellow on leave September 1974–June 1975 from Cornell University, Ithaca, N. Y. 14850

[1]S. B. Trickey, W. P. Kirk, and E. D. Adams, Rev. Mod. Phys. 44, 668 (1972).

[2]W. P. Kirk and E. D. Adams, Phys. Rev. Lett. 27, 392 (1971).

[3]J. M. Dundon and J. M. Goodkind, Phys. Rev. Lett. 32, 1343 (1974).

[4]W. P. Halperin, C. N. Archie, F. B. Rusmussen, R. A. Buhrman, and R. C. Richardson, Phys. Rev. Lett. 32, 927 (1974).

[5]Yu. D. Anufriyev, Zh. Eksp. Teor. Fiz., Pis'ma Red. 1, 1 (1965) [JETP Lett. 1, 155 (1965)].

[6]G. C. Straty and E. D. Adams, Rev. Sci. Instrum. 40, 1393 (1969).

[7]W. P. Halperin, private communication. We have used $T_0 = 16.88$ mK and $P_0 = 3.378\,30$ MPa. Our pressure calibration was adjusted so that the A transition in the liquid for $B = 0$ occurs at $P_A = 3.434\,20$ MPa.

[8]W. R. Abel, A. C. Anderson, W. C. Black, and J. C. Wheatley, Phys. Rev. 147, 111 (1966).

[9]R. A. Scribner, M. F. Panczyk, and E. D. Adams, J. Low Temp. Phys. 1, 313 (1969); E. R. Grilly, *ibid.* 4, 615 (1971).

[10]D. D. Osheroff, R. C. Richardson, and D. M. Lee, Phys. Rev. Lett. 28, 885 (1972).

[11]A. Landesman, J. Phys. (Paris), Colloq. 31, C3-55 (1970); L. J. de Jongh and A. R. Miedema, Advan. Phys. 33, 1 (1974).

Pauling's Ionicity and Charge-Density Waves in Layered Transition-Metal Dichalcogenides

A. H. Thompson

Corporate Research Laboratories, Exxon Research and Engineering Company, Linden, New Jersey 07036

(Received 7 November 1974)

The crystal distortions commonly observed in the layered transition-metal dichalcogenides have been attributed to a Fermi-surface instability, i.e., a charge-density wave. I find that the temperatures of these distortions correlate with the ionicity of the metal-chalcogen bond. This results suggests that these distortion temperatures can be specified without knowing the details of the Fermi surface.

The layered transition-metal dichalcogenides and their intercalation complexes have received much attention as a result of their highly anisotropic properties.[1] Quite apart from the anisotropies, the disulfides and diselenides of Ta and Nb are unstable at lower temperatures and undergo crystal distortions. The discovery of magnetic anomalies associated with these distortions was made by Quinn, Simmons, and Banewicz[2] in their studies of $2H$-$TaSe_2$. Lee *et al.*[3] measured the transport and magnetic properties of $2H$-$TaSe_2$ and $2H$-$NbSe_2$. Ehrenfreund *et al.*[4] showed that the magnetic and transport anomalies are not associated with magnetic ordering as originally suggested,[2] but most likely with subtle crystal distortions.

More recently, many new transitions have been discovered (see Table I) and a mechanism for the distortions has been proposed independently by Williams, Parry, and Scruby,[5] and by Wilson, DiSalvo, and Mahajan.[6] These authors cite electron diffraction evidence to support their propos-